Monte Carlo Studies of Charge-Exchange First Wall Heat Fluxes from the TDF Neutral Beams

L. John Perkins

June 1983

UWFDM-453

FUSION TECHNOLOGY INSTITUTE

UNIVERSITY OF WISCONSIN

MADISON WISCONSIN

Monte Carlo Studies of Charge-Exchange First Wall Heat Fluxes from the TDF Neutral Beams

L. John Perkins

Fusion Technology Institute
University of Wisconsin
1500 Engineering Drive
Madison, WI 53706

http://fti.neep.wisc.edu

June 1983

UWFDM-453

MONTE CARLO STUDIES OF CHARGE-EXCHANGE FIRST WALL HEAT FLUXES FROM THE TDF NEUTRAL BEAMS

L. John Perkins

Fusion Engineering Program
Nuclear Engineering Department
University of Wisconsin
Madison, WI 53706

June 1983

UWFDM- 453

ABSTRACT

Monte Carlo methods are employed to compute surface heat fluxes at the first wall of the Fusion Technology Demonstration Facility (TDF) resulting from charge-exchange of the central cell neutral beams with the fusion plasma. The full 3-dimensional nature of the anisotropic interaction processes of neutral beams with a mirror-confined plasma is retained in the calculations and the resulting surface heat fluxes are mapped both azimuthally and axially on a first wall detector grid. For a total incident beam power of 32.4 MW at each end of the central cell, 4.2 MW is lost as charge exchange neutrals to the first wall. The angular distribution of heat fluxes at the first wall show strong backward peaking with maximum power densities of $\sim$ 2.4 kW cm^{-2} occuring at $\sim$ 180° relative to the incident beam direction. Physical arguments are presented for the behavior of these heat flux distributions in terms of the plasma and beam parameters of the system. Finally, the effectiveness of reducing these high peak power densities to acceptable levels by increasing the first wall radius from 25 cm to 50 and 75 cm is demonstrated.

TABLE OF CONTENTS

1. INTRODUCTION

The Fusion Technology Demonstration Facility (TDF) is a recently completed conceptual design study[1] of a fusion engineering test facility based on the tandem mirror principle. TDF would be a small (18 MW fusion power) driven device ($Q \approx 0.25$) and would produce high first wall neutron fluences (~ 5 MW-y/m^2) at a reasonable capital cost ($\sim 10^3$ M\$) for purposes of providing essential fusion engineering data. A cross section of the device is shown in Fig. 1. A total of 64.8 MW of neutral beam power comprising a 50:50 species mix of deuterium and tritium is injected continuously into the central cell at a beam voltage of 80 kV. A total of eight beamlines, four at each end of the central cell, provide the required current of 1080 A at an average beam energy of 60 keV. The principal parameters of these central cell beams are given in Table 1.

Of the 32.4 MW of neutral beam power injected at each end of the central cell, a fraction will be ionized and trapped in the plasma. The remaining neutrals either penetrate with no interaction and are absorbed by the beam dumps or undergo charge exchange with the plasma ions. The secondary neutral atoms formed in the charge exchange (CX) process will either escape and impact the first wall or undergo ionization or further CX interactions with the plasma. Therefore, from considerations of particle and energy balance, a fraction of the incident beam power is absorbed in the plasma, a fraction escapes as shine-through to the beam dumps and the remainder appears as charge exchange neutral bombardment of the surrounding first wall. Depending on the beam and plasma parameters, the CX neutral power to the first wall can be a significant fraction of the incident beam power and may dictate the need for sophisticated first wall surfaces capable of sustaining high heat fluxes.

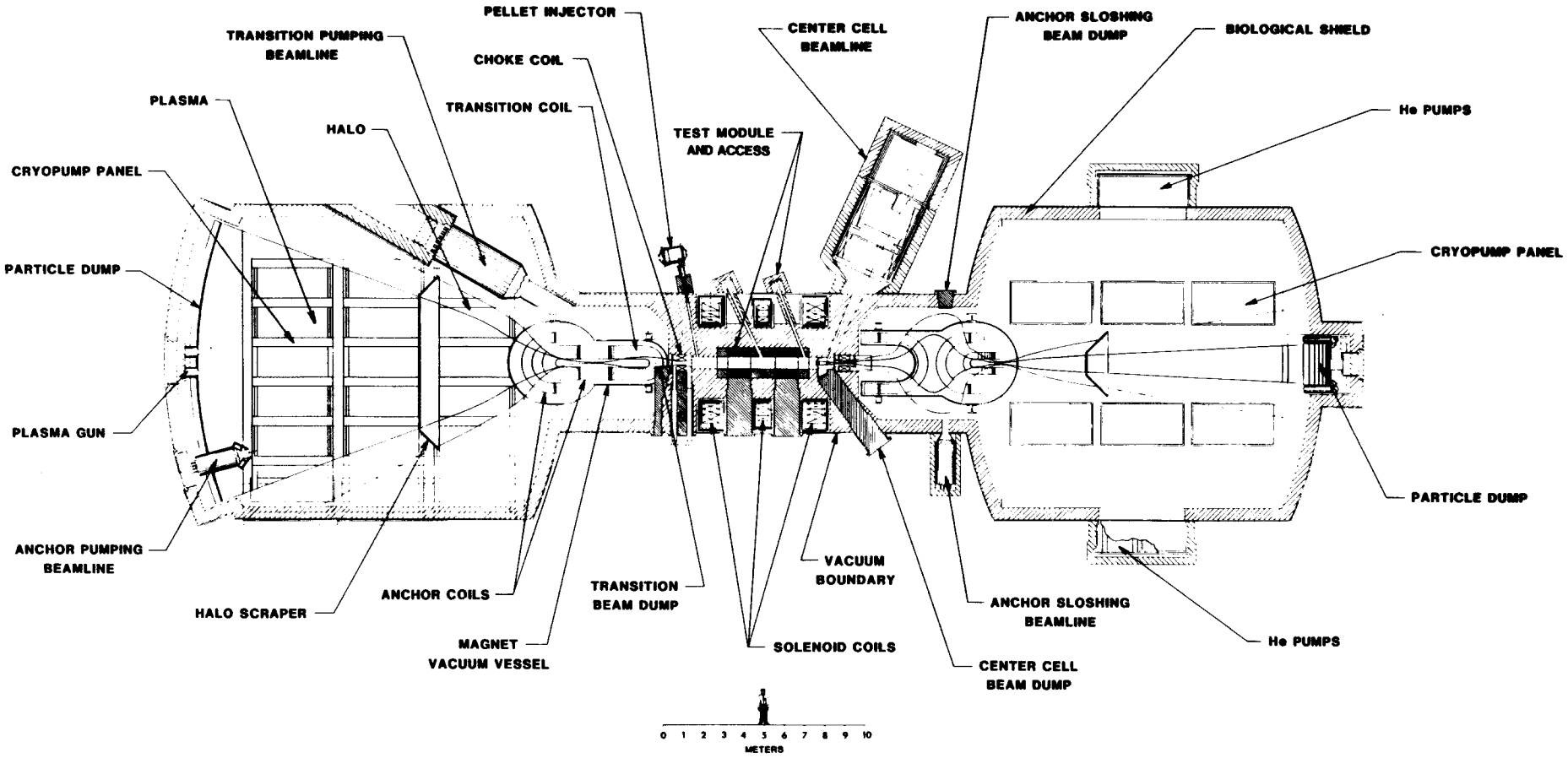

Fig. 1 The Fusion Technology Demonstration Facility (TDF).

Therefore, it is important to accurately predict the power density distribution of the CX flux over the first wall surface.

Table 1. Principal Parameters for the TDF Central Cell Neutral Beams
(Parameters are for both ends of the machine)

Total incident beam power	64.8 MW
Beam voltage	80 kV
Beam species	D, T (50:50)
Total injected current	1080 A
Beam fractions (full, 1/2, 1/3 energy components)	55%, 29%, 16%
Average beam energy	60 keV
Total number of central cell beams	8
Number of beams at each end of central cell	4
Beam injection angle	65°
Angle between four beams at each end	50°

Modeling the steady-state neutral-beam/plasma/wall system in three spatial dimensions is, in general, a very complex process. In the past, various analytical and numerical investigations have been performed which have incorporated various simplifying assumptions regarding system parameters (see, for example, Refs. 2 and 3). However, if one wishes to formally investigate charge exchange phenomena in a 3-dimensional system and retain those phase-space anisotropies inherent in the interaction of a neutral beam with mirror-confined plasmas, then recourse is necessary to Monte Carlo methods.[4,5] Accordingly, a Monte Carlo neutral beam interaction code MCNEUT was adapted and employed to model CX production and transport for the TDF central cell beams. In addition to computing general particle and power balances for neutral beam interaction, CX power density distributions were mapped over the first wall surface in both the axial and azimuthal directions.

2. MONTE CARLO MODELING OF THE TDF BEAM-PLASMA INTERACTION

The Monte Carlo code MCNEUT was originally written at Lawrence Livermore National Laboratory for the purpose of modeling the energy spectra and spatial origination positions of CX fluxes in the 2XIIB minimum-B mirror device.[6] The code was configured for single-species beams on single-species plasmas and has been modified here to accommodate multi-species beams on multi-species plasmas and to allow for more than one incident beam direction.

In the code, a large number of neutral particle histories are followed in three dimensions from their emission from the neutral beam injector through a target plasma which is represented by a bi-Maxwellian distribution function in steady state. Ionization and CX events are simulated by Monte Carlo techniques and descendent generations of neutrals are followed until each particle is either ionized and integrated into the background plasma or escapes and bombards the first wall. Further details on the updated code and its general application to computation of first wall CX power densities can be found in Ref. 5.

In the application of MCNEUT to the TDF central cell neutral beams, the plasma was modeled as a cylinder of 5 m length and 0.10 m radius. The 5 m length was not intended to represent the physical length of the TDF plasma but merely to provide sufficient axial extent such that end effects could be neglected for the beam interaction processes. Four 80 keV neutral beams spaced 50° apart were configured to subtend an angle of 65° relative to the z-axis of the machine with an intersection at the midpoint of the 5 m long cylindrical plasma, 2.5 m from one end. For convenience, this intersection point will be designated as $z' = 0$ for defining the axial location of CX flux distributions and should not be confused with the conventional $z = 0$ datum coordinate at the

center mid-plane of the machine. The target plasma was portioned radially into 32 annular zones in each of which the plasma properties were assumed constant. Escaping CX neutrals were scored on a cylindrical first wall detector grid with 32 azimuthal bins in the θ direction and 20 axial bins in the z' direction; the bin widths were $\Delta\theta = 10°$ and $\Delta z' = 5$ cm, respectively.

A summary of the principal plasma, beam and first wall parameters employed as input parameters to the Monte Carlo code is given in Table 2. Note that here the plasma density profile is modeled as a Gaussian whereas the TDF density profile is legislated[1] to be cubic with a plasma radius of 10 cm. Accordingly, the scale length of the Gaussian profile was chosen such that, when normalized to the same peak (on-axis) number density and some radial cutoff, both profiles yielded the same plasma number density per unit length in the z-direction. One other feature should be noted from Table 2, in that the incident beams are modeled as right-circular cones emanating from point sources with a divergence half-angle defining the standard deviation of a Gaussian beam profile. The distance from each beam point source to the $z' = 0$ point on axis was chosen such that, with a divergence half-angle equivalent to the expected beam divergence ($\sim 0.4°$), less than 1% of the beam footprint fell outside the plasma diameter.

3. RESULTS

3.1 Particle and Power Balances

Table 3 provides a summary of the overall particle and power balances as determined by MCNEUT for those input parameters shown in Table 2. Note that these results are for the four beams at one end of the machine. Note

Table 2. Principal Input Parameters to the Monte Carlo Code

Number of C.Cell beams (each end)	4
Injection angle	65°
Angle between beams	50°
Beam voltage	80 kV
Beam fractions	55%, 29%, 16%
Beam species	D/T (50:50)
Injected current per beam	135 A
Total injected current (each end)	540 A
Beam profile	Gaussian
Beam source - plasma distance	5.55 m
Beam half angular divergence	0.4°
Plasma length	5 m (cylindrical)
Beam intersection point ($z' = 0$)	2.5 m from one end
Plasma radius	10 cm
Plasma profile	Gaussian
Plasma radial scale length	10.087 cm
Plasma density	6.5×10^{14} cm^{-3}
T_{perp} 34 keV	
$T_{parallel}$	4 keV
T_e 2.1 keV	
On-axis B field	4.5 T
Number of annular plasma zones	32
Plasma radial zone width	0.3125 cm
Radius of first wall	25 cm (cylindrical)
Dimensions of first wall detector grid	32 x 20
Grid azimuthal bin width ($\Delta\theta$)	10°
Grid axial bin width ($\Delta z'$)	5 cm
Number of neutral histories	40,000

Table 3. Particle and Power Balances for the TDF Central Cell Beams

(Results for four beams at one end of the central cell)

Particle Balance	
Incident current	$3.371 \times 10^{21}\ s^{-1}$
Trapping fraction[a]	0.9894
Total trapped current[b]	$3.335 \times 10^{21}\ s^{-1}$
Net trapped current[c]	$2.737 \times 10^{21}\ s^{-1}$
Power Balance	
Incident power	32.40 MW
Shine-through power to dumps	0.343 MW
CX power to walls	4.203 MW
Net trapped power	27.85 MW

Notes:

a. Fraction of incident particles which undergo at least one interaction (CX or ionization) with the plasma.

b. Number of particles per second which undergo at least one interaction (CX or ionization) with the plasma.

c. Number of particles per second which are ionized and become trapped in the plasma. This is equivalent to a fueling rate.

carefully the definitions of trapping fraction, total trapped current and net-trapped current. The Monte Carlo statistics for these integral quantities are $\lesssim$ 0.6%.

It should be noted from Table 3 that the ratio of the net trapped current to incident current is not equal to the ratio of the net trapped power to the incident power. This is because an incident beam particle of fixed energy can charge exchange with plasma ions having a distribution of energies. Since some of these secondary neutrals can charge exchange or escape before becoming ionized, this will, in general, result in a plasma energy trapping which does not scale directly with the particle trapping. Note also that these particle and energy balances will not necessarily precisely agree with those computed in the earlier physics phase of the machine design[1] due to differences in both computational technique (Monte Carlo rather than an analytic-numerical method) and modeling of the neutral beam footprint (conical Gaussian beam with a footprint of ~ 0.14 m diameter rather than a rectangular Gaussian beam with a footprint of ~ 1 x 0.14 m).

3.2 Spatial Variation of CX Power Densities on First Wall Surface

Besides the integral quantities in Table 2, charge exchange power density distributions were obtained at the 32 x 20 detector grid on the first wall surface. Figure 2 is a polar plot of the CX power density distribution in the xy plane for one of the four beams at a z' value of -0.025 m; i.e. this is the azimuthal variation of CX power density over the first wall at an axial position displaced 2.5 cm from the beam intersection point at z' = 0. Note the direction of the incident beam is at $\theta = 90°$. Note also that since the beam injection angle is 65°, this incident beam is inclined 25° out of the xy plane of the figure. Figure 3 is the corresponding polar plot when all four beams

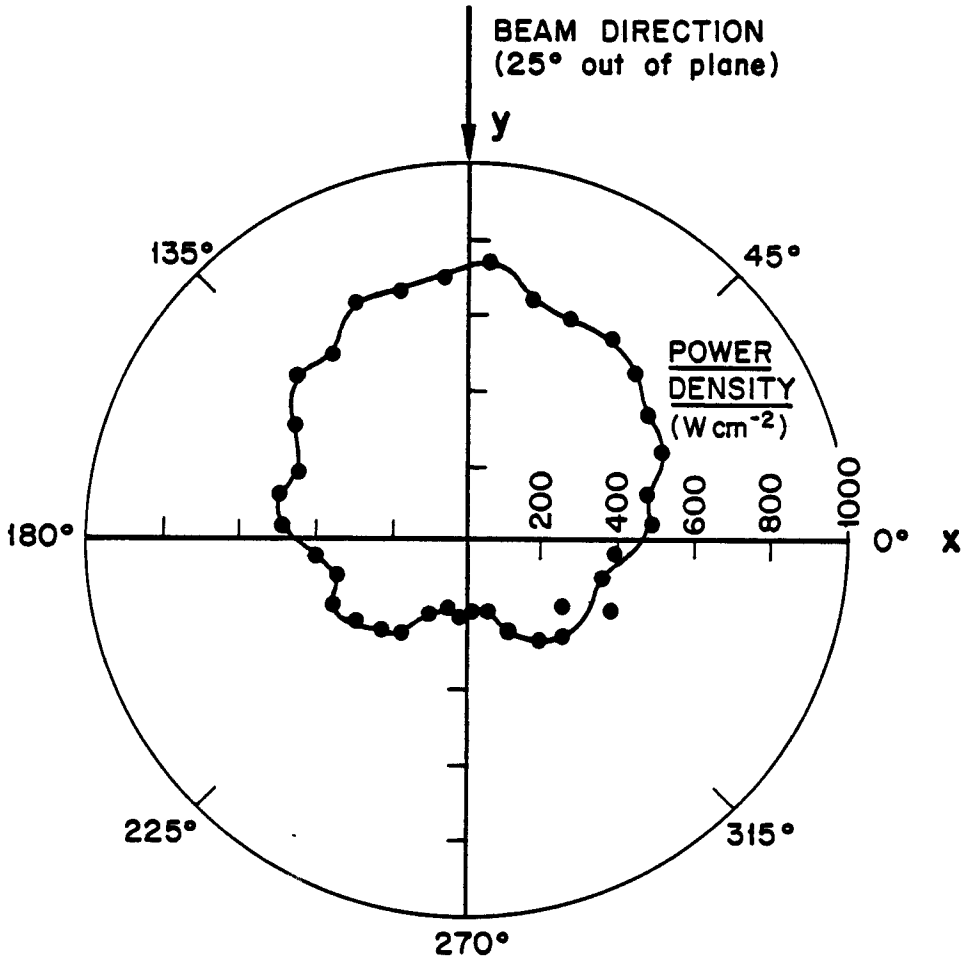

Fig. 2. Polar distribution of charge exchange power density at the first wall for one beam. The axial coordinate is z' = -0.025 m.

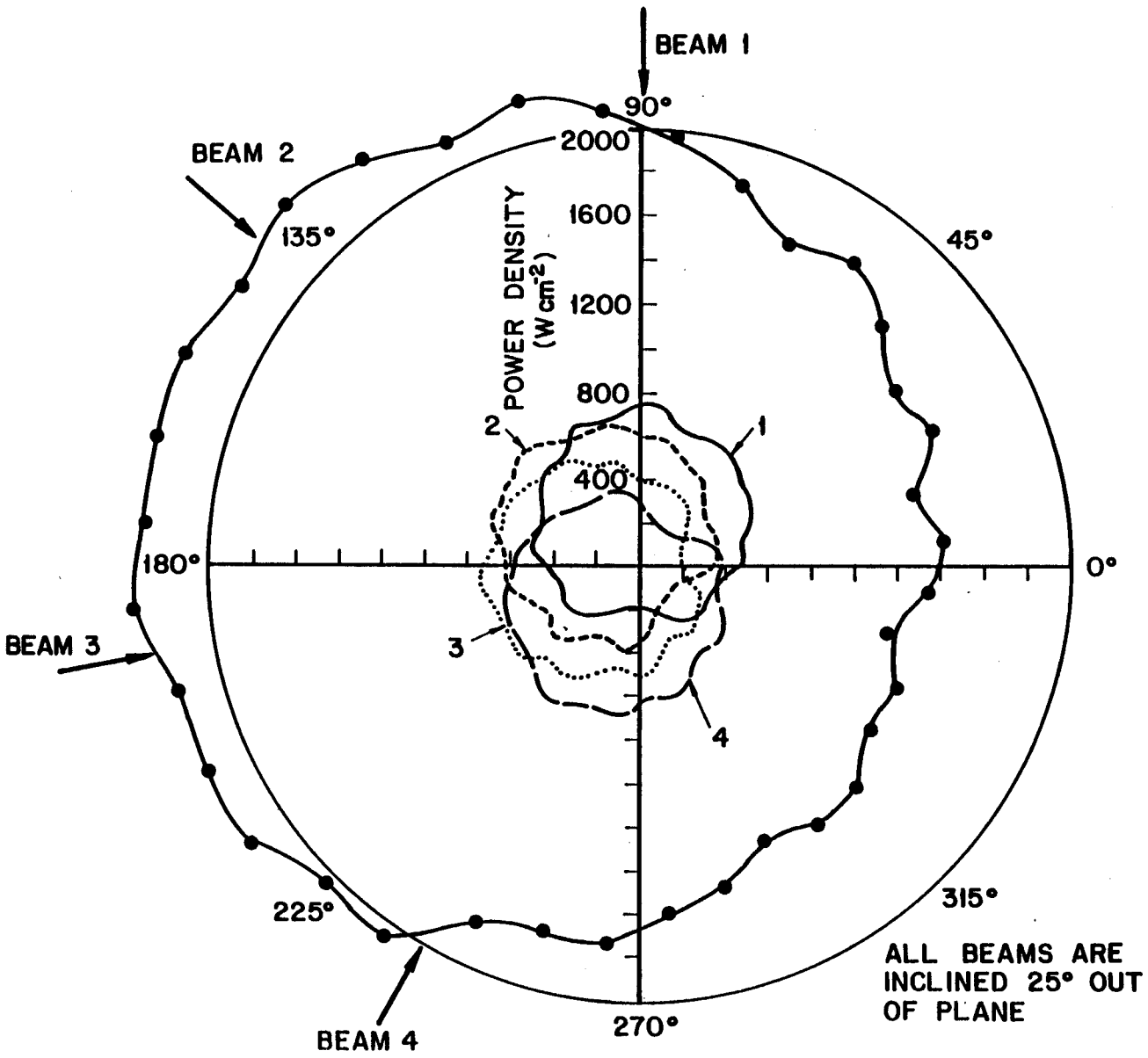

Fig. 3. Composite polar distribution of charge exchange power density at the first wall for four beams. The axial coordinate is z' = -0.025 m.

are included. The four individual distributions are shown as is the composite distribution formed when the individual distributions are superposed. The maximum power density is seen to be ~ 2369 W cm^{-2} at θ = 185°, clearly a very high heat load!

From the code output, it is possible to construct polar plots similar to Fig. 3 for each of the 20 axial grid positions along the first wall surface. However, it is more instructive here to pre-process this data and select only the maximum, minimum and average CX power densities at each axial position and plot these as a function of the corresponding z' coordinate. Accordingly, these data are shown in Fig. 4. Peak values of the maximum, average and minimum power density distributions are seen to be ~ 2380, 1875 and 1270 W cm^{-2} at the axial positions of z' = -2.5, -1.5 and -0.5 cm, respectively.

4. DISCUSSION OF RESULTS

4.1 Angular Distribution of First Wall Power Densities

One of the major features of the CX wall flux for the single beam shown in Fig. 2 is that the distribution is strongly backward-peaked, i.e. maximum CX power densities occur at ~ 180° relative to the incident beam direction. It is also interesting to note that the distribution is quite symmetric about the y-axis; this is to be expected in view of the incident beam direction. The slight deviations from true symmetry are, of course, attributable to Monte Carlo statistics (~ 6% here).

For the composite polar distribution in Fig. 3, the strong backward peaking of the single beam distribution has been somewhat ameliorated by the superposition of four beams at 50° apart. However, the composite wall flux is still dominant in the general backward direction. Note that when the machine

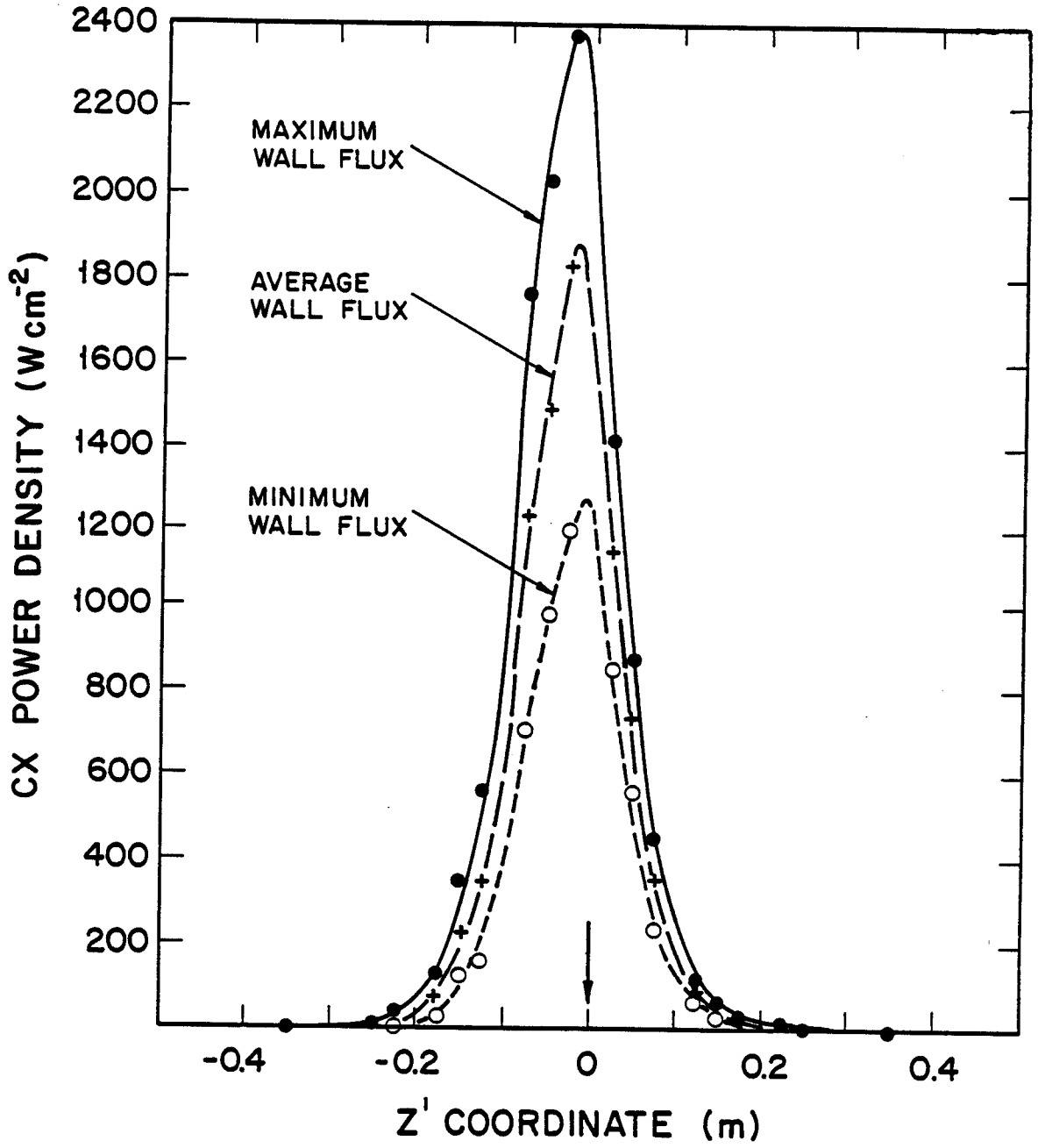

Fig. 4. Axial variation of charge exchange heat loads for a first wall radius of 25 cm. The beam intersection point is at z' = 0.

passes through startup, neutral fluxes will progress from strongly forward-peaked at low plasma densities to being backward-peaked at full plasma conditions.

The backward peaking of the TDF CX distributions should be contrasted with the forward peaking observed[5] for the CX distributions from the transition pumping neutral beams in MARS tandem mirror reactor study.[7] Generally, for a single CX interaction, the product neutral tends to be emitted in the forward direction because the CX cross section is large for particle pairs with small relative velocities.[5] However, those forward-peaked CX neutrals directed into the bulk of a dense plasma have a strong chance of undergoing a further interaction (CX or ionization). In addition, the incident neutral beam will be attenuated exponentially in the plasma, thus the primary CX production rate decreases along the chord length of the incident beam through the plasma. Therefore, in general, for a high energy neutral beam and/or low plasma line density, the polar CX wall distribution tends to be forward-peaked. Conversely, for lower energy beams and/or higher plasma line densities, the wall distribution tends to a maximum in the backward direction. As the beam trapping fraction approaches 100%, strong backward peaking would be expected. This would then account for the backward peaking of the TDF CX wall distributions compared with the forward peaking in the MARS reactor. The MARS plasma density is only 1×10^{14} cm^{-3} compared with 6.5×10^{14} cm^{-3} for TDF. In addition, the MARS neutral beams are 97 keV (negative ion) with no half or third energy components,[7] whereas the TDF beams are 80 keV (positive ion) with appreciable half and third energy components (29% and 16% respectively). Therefore, the bulk of the TDF CX neutrals are produced on the beam side of the plasma and forward directed products are strongly reabsorbed.

4.2 Consequences of High Heat Fluxes from Charge Exchange Interactions

A significant feature of the axial plots of maximum, minimum and average CX power densities in Fig. 4 is the "peakyness" of the distributions. Again, in comparison with the MARS reactor, TDF has considerably less total charge exchange power loss to the walls (4.077 MW each end compared with 19.28 MW for MARS). However, in MARS this power is distributed over a greater axial extent in the z-direction resulting in lower peak values of the maximum wall flux ($\sim$ 705 W cm^{-2} compared with 2380 W cm^{-2} here for TDF). Again, this can be explained by reference to the different beam/plasma conditions discussed above and, additionally, by noting that T_{perp} and $T_{parallel}$ in MARS are 58 and 59.5 keV, respectively, compared with 34 and 4 keV in TDF. Clearly, in the case of TDF there is a high probability of producing a CX neutral with a direction closely normal to the z-axis. These factors all contribute to the sharpness and the very high peak values of the TDF axial distributions. Further details on CX wall fluxes in the MARS tandem mirror reactor can be found in Ref. 5.

The combination of these high peak CX power densities and predominantly backward-directed emissions is rather unfortunate for TDF. At least in the case of forward-directed distributions such as those for MARS, maximum CX flux densities are directed towards the beam dump surfaces. Clearly, first wall heat loads of nearly 2400 W cm^{-2} are too large for current or near term high-heat-flux technologies. Beam dumps based on the "Hypervapotron" principle are currently being incorporated on the JET tokamak for heat loads of $\sim$ 1-1.5 kW cm^{-2} under quasi steady-state ($\sim$ 20 s) conditions.[8] However, such dumps have a rather bulky configuration and could not conceivably be integrated in the first wall area of TDF where space is at a premium. In practice, heat loads to water-cooled first wall surfaces should be limited to certainly no more

than 500 W cm^{-2}. In the STARFIRE tokamak reactor design for example, maximum surface heat loads to the water-cooled limiter were restricted to ~ 240 W cm^{-2}.[9]

4.3 The Effect of First Wall Radius on CX Heat Loads

As an alternative to reconfiguring beam parameters and/or geometries, the most effective method of reducing the peak heat loads in Fig. 4 to acceptable levels is to simply increase the radius of the first wall from its original value of 25 cm. This would only be necessary in the vicinity of the high CX power densities and would not, therefore, be detrimental to neutron wall loading levels in the bulk of the central cell. Accordingly, in order to assess the effect of recessing the first wall, the beam/plasma parameter set in Table 1 was re-run with two new values of first wall radius, namely 50 and 75 cm.

Figure 5 is a plot of the resulting maximum CX heat loads at each axial position as a function of the z' coordinate for these two new wall radii. Also shown in Fig. 5 for comparison purposes is the axial distribution at the original wall radius of 25 cm extracted from Fig. 4. Note that the peak values have been reduced from ~ 2400 W cm^{-2} for r_w = 25 cm to much more acceptable values of ~ 630 and 290 W cm^{-2} for r_w = 50 and 75 cm, respectively. In fact these reductions are considerably greater than the 1/r scaling expected from a line source and are due to the distributed nature of the CX emission across the plasma volume.

One other interesting feature of Fig. 5 is that the wall fluxes at the wings of the distributions are actually greater for the larger wall radii. This can be explained as follows. Consider those CX neutrals which are produced by neutral beam interactions in a given xy plane and which are emitted at large angles relative to this plane. If these neutrals are to contribute

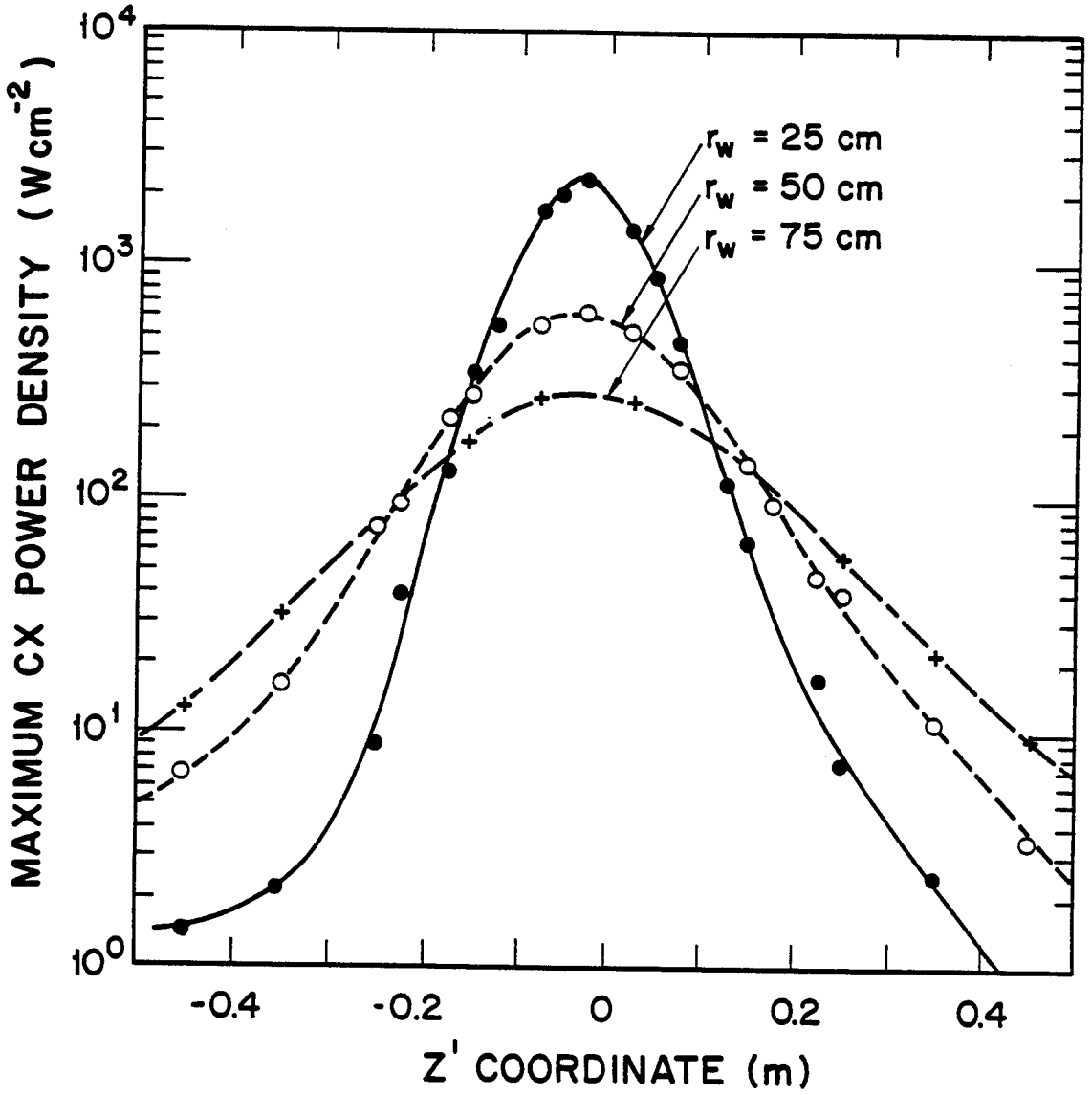

Fig. 5. Effect of first wall radius on the axial variation of maximum charge exchange heat loads.

to the CX flux at a given z' coordinate in the wings of the distribution, they must travel through a larger plasma chord length to bombard the wall at the smaller radii than when bombarding the larger wall radii at the same z' coordinate. Thus for z' coordinates sufficiently far from z' = 0, the apparent loss in intensity due to increased wall radius is compensated by lower attenuation within the plasma. Therefore, in the wings of the CX flux distributions it is preferable to keep the wall radius relatively small.

5. CONCLUSIONS

In conclusion, Monte Carlo calculations have shown that peak charge exchange power densities from the TDF central cell neutral beams will be in the vicinity of 2400 W cm^{-2} for a first wall radius of 25 cm. The heat loads have a predominantly backward-peaked distribution. The total charge exchange power loss from the plasma is 4.2 MW at each end of the device. One effective method of reducing the peak power densities to the first wall is to increase the wall radius from 25 cm to at least 75 cm in the vicinity of z' = 0 and taper it back to 25 cm at axial coordinates where heat loads have fallen to acceptable levels. In this latter design, maximum charge exchange heat loads are less than 300 W cm^{-2} and could be accommodated by reasonably conventional water-cooled first wall designs.

ACKNOWLEDGEMENTS

The author is pleased to acknowledge the advice and assistance of Drs. T.B. Kaiser and J.E. Osher of Lawrence Livermore National Laboratory.

This research is supported by the U.S. Department of Energy, Office of Fusion Energy.

REFERENCES

1. J. Doggett et al., "Fusion Technology Demonstration Facility (TDF)," UCID-19328, Lawrence Livermore National Laboratory (to be published 1983).

2. J. Hovingh and R.W. Moir, "Efficiency of Injection of Neutral Beams in Thermonuclear Reactors," Nuclear Fusion 14, 629 (1974).

3. G.A. Carlson and G.W. Hamilton, "Wall Bombardment Due to the Charge Exchange of Injected Neutrals with a Fusion Plasma," UCRL-75306, Lawrence Livermore Laboratory (1974).

4. R.L. Miller, "Monte Carlo Simulation of Neutral Beam Injection for Mirror Fusion Reactors," Ph.D. Thesis (University of Illinois, 1979).

5. L.J. Perkins and T.B. Kaiser, "Monte Carlo Studies of Charge-Exchange First Wall Heat Loads from Neutral-Beam Injection in Tandem Mirror Fusion Reactors," University of Wisconsin Fusion Engineering Program Report (to be published, 1983).

6. T.B. Kaiser, MFE Quarterly Report, UCRL-50551-77-4, Lawrence Livermore National Laboratory (1978).

7. "Mirror Advanced Reactor Study (MARS) - Interim Design Report," UCRL-53333, Lawrence Livermore National Laboratory (1983).

8. "Joint European Torus (JET) Annual Report," JET Joint Undertaking (1981).

9. C.C. Baker et al., "STARFIRE - A Commercial Tokamak Fusion Power Plant Study," ANL/FPP-80-1, Argonne National Laboratory (1980).